Journal of King Saud University - Science 36 (2024) 103111

HOSTED BY

Contents lists available at ScienceDirect

Journal of King Saud University - Science

journal homepage: www.sciencedirect.com

Full Length Article

Isolation and characterization of the lytic bacteriophages and their application in combination with amoxicillin against *Aeromonas dhakensis*

Thanchanok Sawaengwong [a], Sirinthorn Sunthornthummas [b], Rinratree Wongyoo [a], Komwit Surachat [c,d], Achariya Rangsiruji [e], Thassanant Atithep [f], Siriruk Sarawaneeyaruk [a], Katsumi Doi [g], Kwannan Nantavisai [h], Kedvadee Insian [a], Rattanaruji Pomwised [i], Onanong Pringsulaka [a,*]

[a] Department of Microbiology, Faculty of Science, Srinakharinwirot University, Bangkok 10110, Thailand
[b] National Biobank of Thailand (NBT), National Science and Technology Development Agency, Pathum Thani 12120, Thailand
[c] Department of Biomedical Sciences and Biomedical Engineering, Faculty of Medicine, Prince of Songkla University, Hat Yai, Songkhla 90110, Thailand
[d] Translational Medicine Research Center, Faculty of Medicine, Prince of Songkla University, Hat Yai, Songkhla 90110, Thailand
[e] Department of Biology, Faculty of Science, Srinakharinwirot University, Bangkok 10110, Thailand
[f] Frontier Research Center (FRC) Vidyasirimedhi Institute of Science and Technology (VISTEC), Wangchan Valley, Rayong 21210, Thailand
[g] Laboratory of Microbial Genetic Technology, Department of Bioscience and Biotechnology, Graduate School of Agriculture, Kyushu University, Fukuoka 812-8581, Japan
[h] Department of Microbiology, Faculty of Medicine, Srinakharinwirot University, Bangkok 10110, Thailand
[i] Division of Biological Science, Faculty of Science, Prince of Songkla University, Songkhla, Hat Yai, 90110, Thailand

ARTICLE INFO

Keywords:
Aeromonas dhakensis
Phage–antibiotic synergy
Phage therapy
Genome analysis

ABSTRACT

Aeromonas dhakensis stands out as the most potent *Aeromonas* species causing a range of human diseases. This research marks the pioneering effort in isolating and characterizing virulent phages targeting *A. dhakensis*. Only the AM isolate among the *Aeromonas* isolates showed compatibility for phage isolation and was identified as *A. dhakensis*. Computational analysis identified the presence of virulence factors and antimicrobial resistance genes in *A. dhakensis* AM. Phage isolation was conducted using this particular strain as the host, resulting in the isolation of four virulent phages: vB_AdhM_DL, vB_AdhS_TS3, vB_AdhM_TS9, and vB_AdhS_M4. Bacterial numbers significantly decrease after both pre-treatment and post-treatment with individual phages and phage cocktails, ranging from 2.82 to 6.67 log CFU/mL and 4.01 to 6.49 log CFU/mL, respectively. Combining a phage cocktail with sub-MIC amoxicillin led to complete inactivation in both pre-treatment and post-treatment scenarios within a 200 μL volume. The complete genomes of phages vB_AdhM_DL, vB_AdhS_TS3, and vB_AdhM_TS9 were determined to be 42,388 bp, 115,560 bp, and 115,503 bp, respectively. This study establishes the effectiveness of using phages as an complement with sublethal antibiotic concentrations, presenting a potential and effective therapeutic approach.

1. Introduction

Aeromonas dhakensis, a member of the *Aeromonas* genus, represents a significant pathogenic species with distinct characteristics and implications for human health. Prior to the identification of *A. dhakensis*, the most prevalent *Aeromonas* species included *A. hydrophila, A. caviae*, and *A. veronii.* However, *A. dhakensis*, formerly synonymous with *A. hydrophila* subsp. *dhakensis* (Huys et al., 2002) and *A. aquariorum* (Martinez-Murcia et al., 2008), presents a unique challenge in identification. Phenotypic methods often misidentify it as *A. hydrophila* (Beaz-Hidalgo et al., 2013), and 16S rRNA sequencing has been deemed unreliable for distinguishing *Aeromonas* species at the species level (Janda and Abbott, 2010). Despite these challenges, *A. dhakensis* has garnered increasing attention due to its capacity to cause a spectrum of infections in humans, including gastroenteritis, wound infections, bacteremia, skin and soft-tissue infections, and respiratory infections (Janda and Abbott, 2010; Beaz-Hidalgo et al., 2013).

A. dhakensis exhibits distinct geographic prevalence, primarily in hot

* Corresponding author.
E-mail addresses: onanong@g.swu.ac.th, opringsulaka@gmail.com (O. Pringsulaka).

https://doi.org/10.1016/j.jksus.2024.103111
Received 7 March 2023; Received in revised form 17 January 2024; Accepted 23 January 2024
Available online 30 January 2024

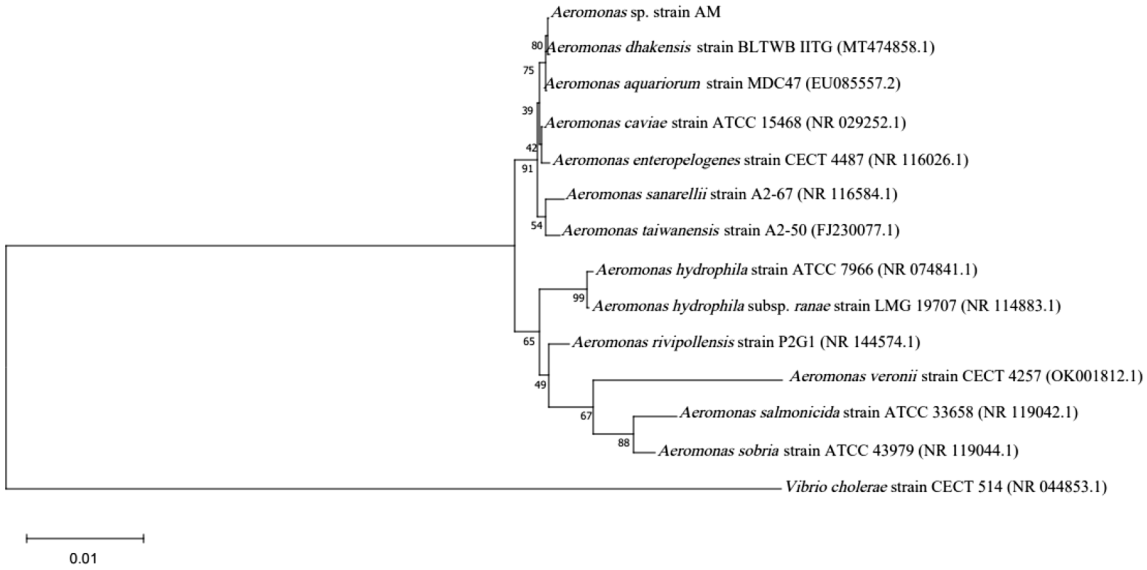

Fig. 1. Phylogenetic tree of *Aeromonas* spp. based on the 16S rRNA gene using neighbor-joining method. Bootstrap values (%) of 1000 replicates are represented on the branches.

Table 1
Biochemical tests of *A. dhakensis* AM.

Biochemical tests	Results
Indole	+
Methyl red	+
Voges-Proskauer	+
Citrate	+
Hemolysis	β
Deoxyribonuclease	+
Gelatinase	+
Catalase	+
Oxidase	+
Oxidative/fermentation glucose test	F
Motility	+
Urease	+
Nitrate	+
TSI (Acid/Alkali)	A/A
Arginine dihydrolase	+
Lysine decarboxylase	+
Ornithine decarboxylase	–
Acid from	
Lactose	–
Sucrose	+
L-arabinose	–
Mannitol	+
Salicin	+

+ represents positive, – represents negative, and F represents fermentation.

climate countries like Bangladesh, Taiwan, Australia, Malaysia, and Thailand (Huys et al., 2002; Chen et al., 2014; Aravena-Roman et al., 2011; Puthucheary et al., 2012; Yano et al., 2015). *A. dhakensis*'s enhanced virulence is attributed to its various virulence factors, including hemolysins and extracellular enzymes, contributing significantly to its invasiveness (Cascon et al., 2000). Clinical strains are found in various anatomical sites, from stool to blood and wounds (Chen et al., 2014). Antibiotics play a vital role in treating *A. dhakensis* infections, yet increasing resistance to agents like amoxicillin, cephalothin, and cefoxitin is concerning (Figueras et al., 2009). Additionally, the biofilm-forming ability of some strains complicates treatment by allowing adherence to surfaces, evading conventional medications. Given these challenges, exploring alternative treatments is crucial.

Bacteriophages are viruses that kill specific bacteria without disturbing other flora. Many studies have isolated phages against *A. hydrophila* and have determined their efficacy for protective and therapeutic effects against disease (Jun et al., 2015; Easwaran et al., 2017; El-Araby et al., 2016). However, there have been few reports on the isolation and characterization of lytic phages specific to *A. dhakensis*. The objective of this study was to isolate and characterize a new lytic phage from water that infects *A. dhakensis*. This study also investigated the lytic activity of the isolated phage and its combination with antibiotics against *A. dhakensis in vitro*.

2. Materials and methods

2.1. Isolation of Aeromonas

To isolate *Aeromonas* species, 30 samples were collected from different sources, including fishponds, canal water, and rivers in Bangkok, Thailand. The samples were streaked onto an *Aeromonas* isolation medium (HiMedia, India) supplemented with ampicillin. The plates were incubated for 24 h at 30 °C. The dark green colonies resembling *Aeromonas* sp. were selected. Gram-negative bacteria capable of degrading nitrates to nitrites, glucose fermenters, oxidase, and catalase-positive isolates resembling the genus *Aeromonas* were selected for 16S rRNA gene sequencing analysis. Other biochemical tests were used to differentiate between *Aeromonas* genera. L-arabinose fermentation was also differentiated between *A. hydrophila* and *A. dhakensis*. Likewise, salicin fermentation allowed differentiation between *A. hydrophila* and *A. dhakensis* from *A. hydrophila* subsp. *ranae* (Beaz-Hidalgo et al., 2013).

2.2. Identification of Aeromonas spp

The genomic DNA obtained from the *Aeromonas* isolate underwent extraction utilizing the AccuPrep® Genomic DNA Extraction Kit (Bioneer, Korea) and was employed as templates for PCR amplification. The 16S rRNA gene was amplified using a pair of universal primers, 27F (5′-AGAGTTTGATCCTGGCTCAG-3′) and 1492R (5′-GGCTACCTTGTTACGACTT-3′) as described by Lane (1991). Subsequently, the sequenced fragments were compared to the GenBank database through the Basic Local Alignment Search Tool (BLAST), and phylogenetic trees were constructed using the neighbor-joining method in the MEGA 5.1 software package.

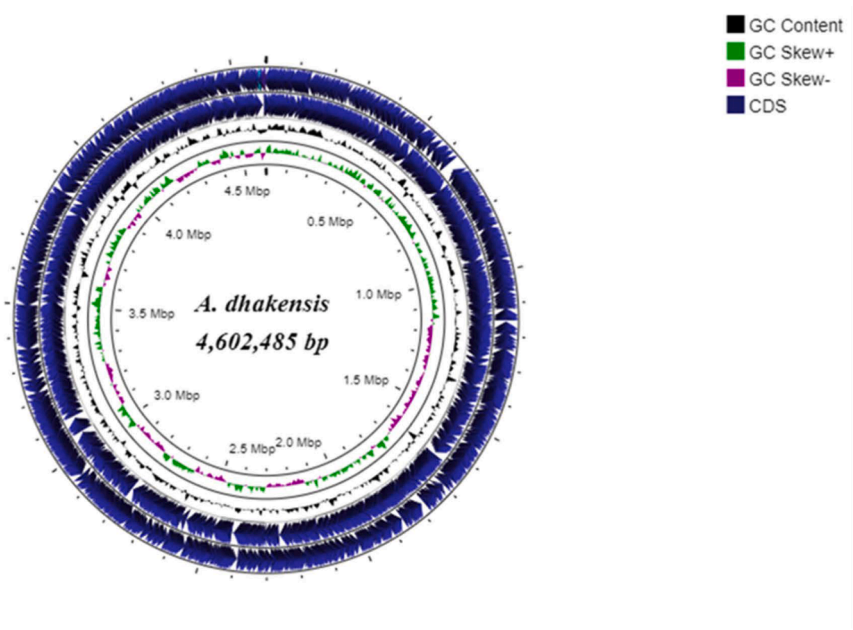

Attribute	*A. dhakensis* AM value
Genome size (bp)	4,602,485
Number of contigs	118
N50	125671
L50	11
GC content (%)	61.9
Number of coding sequences	4256
Number of RNAs	130
Antimicrobial resistance)AMR(gene	8
Prophage	5
Virulence genes	137
GenBank accession	JAPHNH000000000
BioSample accession	SAMN31666460
BioProject accession	PRJNA899678

Fig. 2. Genome features of *A. dhakensis* AM. Circular representation of the following characteristics are shown from the outside to the center of the diagram. Circle 1: coding sequence (CDS) on the reverse strand, circle 2: coding sequence (CDS) on the forward strand, circle 3: GC contents, circle 5: GC skew values (GC skew + shown in green, GC skew- shown in pink).

2.3. Antimicrobial susceptibilities of Aeromonas isolates

Aeromonas isolates were underwent MIC testing using MIC test strips, which included amoxicillin, chloramphenicol, doxycycline, gentamicin, and tetracycline (Liofilchem® MTS™, Italy). The interpretative criteria were in accordance with the Clinical and Laboratory Standards Institute (CLSI) VET04 guidelines (CLSI, 2020).

2.4. Phage isolation and detection

The isolated *Aeromonas* strains served as hosts for bacteriophage isolation, following the method described by Sunthornthummas et al. (2017). The presence of phages was determined using the double-layer agar plate method on NA medium. Phage plaques were counted following an overnight incubation at 30 °C and expressed as plaque-forming units (PFU/mL).

2.5. Electron microscopy

Phage morphology was visualized by transmission electron microscopy (TEM) using carbon-formvar-coated grids, 1% (w/v) uranyl acetate staining (pH 4.5), and a TECNAI 20 TWIN transmission electron microscope operating at 120 kV with a magnification of 120,000×.

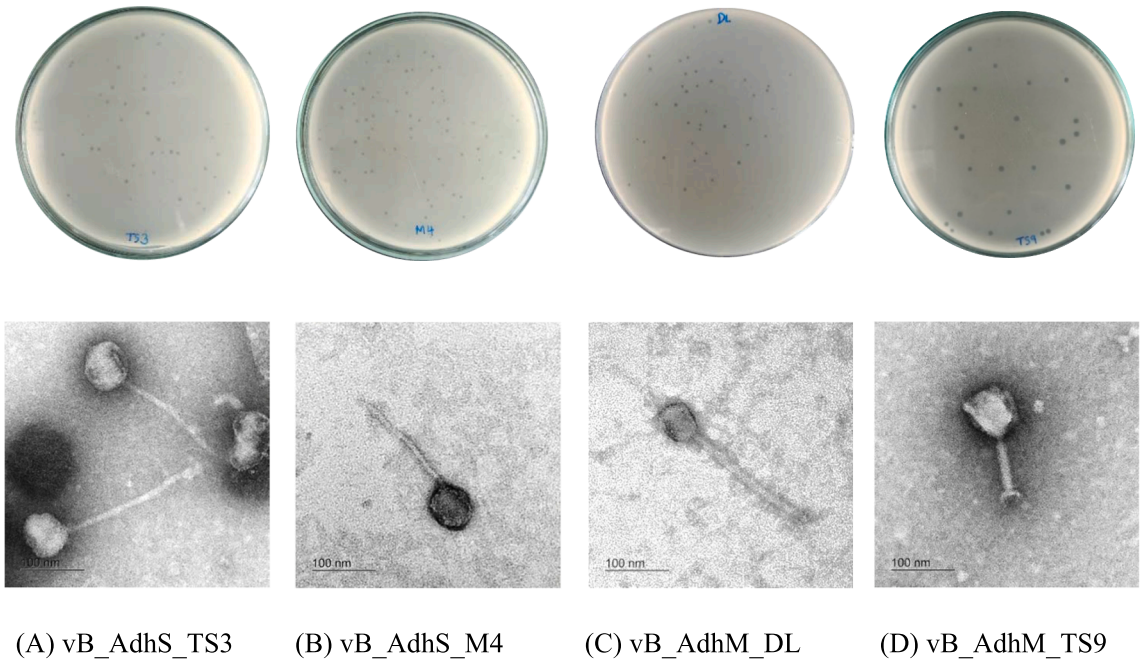

Fig. 3. Plaques and TEM images of phage vB_AdhS_TS3 (A), vB_AdhS_M4 (B), vB_AdhM_DL (C), and vB_AdhM_TS9 (D). Scale bar = 100 nm.

2.6. Host-range determination and determination of optimal multiplicity of infection (MOI)

The host range of the isolated phages was determined using the spot test method. Other reference strains of *Aeromonas* were tested for susceptibility to phages. Bacterial sensitivity to the phage was indicated by the presence of a plaque at the spot. Additionally, a host strain suspension (10^8 CFU/mL) in NB was mixed with the phage stock at four different ratios (0.01, 0.1, 1, and 10 PFU/CFU) to determine the optimal MOI. The ratio with the highest phage titer was considered the optimal MOI (Pringsulaka et al., 2011).

2.7. One-step growth curve experiments

A one-step growth curve for each phage isolate was performed as Sunthornthummas et al. (2017). The latent period, rise period, and burst size were calculated using the one-step growth curve (Adams, 1959).

2.8. pH and thermal stability

For the pH stability tests, NB was pre-adjusted to a range of pH values (pH 2.0–11.0). A phage suspension (10^{10} PFU/mL) was inoculated and incubated for 90 min at 30 °C. For thermal inactivation experiments, phage lysates (10^{10} PFU/mL) were subjected to heat treatment at 4, 30, 37, 45, 63, 72, and 100 °C in NB. The phage titer was determined using the double-layer agar plate method for both the pH stability tests and thermal inactivation experiments.

2.9. Whole genome sequencing and computational analyses

2.9.1. DNA extraction and sequencing

Genomic DNA of *Aeromonas* sp. AM was extracted using an AccuPrep Genomic DNA Extraction Kit (Bioneer, Daejeon, Korea). Phage DNA was isolated as previously described (Sunthornthummas et al., 2017). The purified genomic DNA was sent to the Beijing Genomics Institute (BGI) in China for short-read sequencing.

2.9.2. Genome assembly and annotation

De novo assembly of *Aeromonas* sp. AM and three phage genome sequences were constructed using SPAdes 3.12 (Bankevich et al., 2012). The examination of read quality was conducted using FASTQC (Brown et al., 2017), and trimming was performed using Trimmomatic 0.39 (Bolger et al., 2014). Functional annotation was performed using Prokka v1.14 (Seemann, 2014).

2.9.3. Bioinformatics analyses

Nucleotide and amino acid sequences were compared using Blastn software. Translated open reading frames (ORFs) were compared to the non-redundant GenBank protein database using the Blastp software. To further improve the annotation of predicted proteins, we utilized tools such as the hhpred server (https://toolkit.tuebingen.mpg.de/tools/hhpred). Additionally, the genomic DNA of *A. dhakensis* AM and three phages was screened for the presence of virulence genes using the Virulence Factors of Pathogenic Bacteria (VFDB) (Liu et al., 2022a), PlasmidFinder 2.1 (Carattoli et al., 2014), Comprehensive Antibiotic Resistance Database (CARD) databases (Alcock et al., 2020), and PHASTER was used to identify prophages in bacterial genomes (Zhou et al., 2011). The genome of *Aeromonas* sp. AM and the three phages were visualized using the CGView webserver (https://beta.proksee.ca/) (Grant and Stothard, 2008).

2.9.4. Accession numbers

The genome sequences of *A. dhakensis* AM were deposited in the NCBI database under accession number JAPHNH000000000, and the genome sequences of phage vB_AdhS_TS3, vB_AdhM_TS9, and vB_AdhM_DL were deposited in the NCBI database under accession number OP820700, OP820701, and OP820702, respectively.

2.10. A. dhakensis growth inhibition by single phage and phage cocktail in vitro

Phage therapy was divided into two treatments: pre- and post-treatment. In the pre-treatment experiment, phages or phage cocktail were added before inoculation with *A. dhakensis* AM (1×10^8 CFU/mL), resulting in MOIs of 0.1, 1, and 10. In the post-treatment experiment, *A. dhakensis* AM suspensions (1×10^8 CFU/mL) were inoculated into NB and incubated for 3 h. Equal volumes of phages or phage cocktail were added at MOIs of 0.1, 1, and 10. Both treatments were performed in a

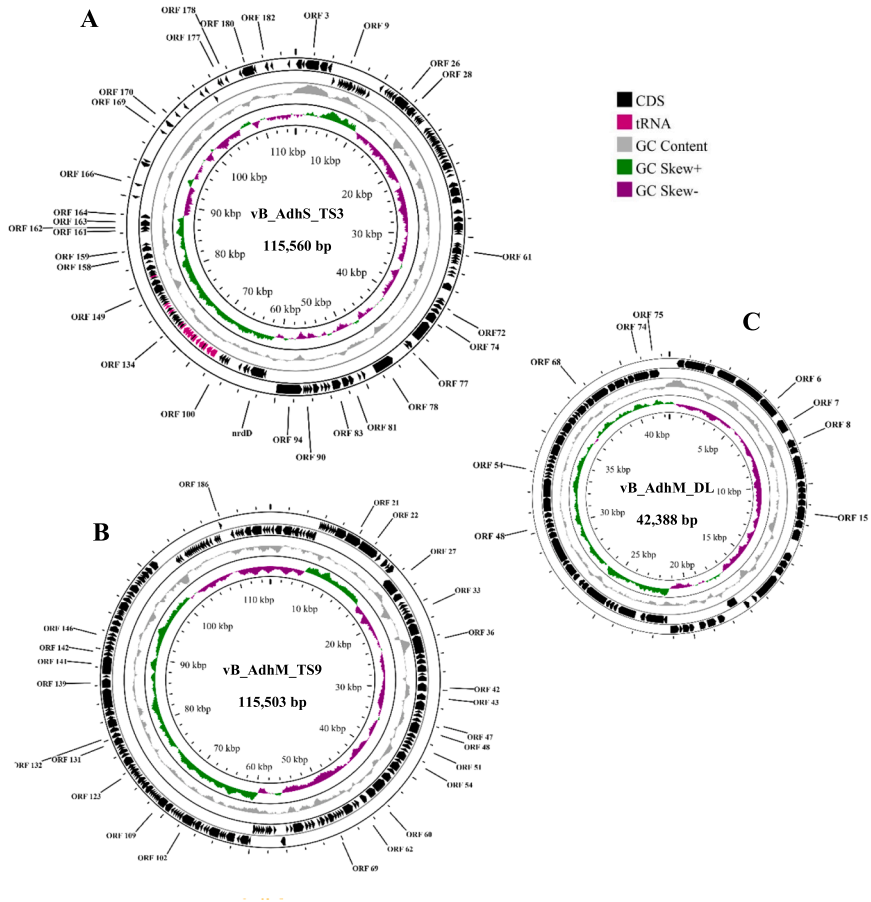

Features	vB_AdhS_TS3	vB_AdhM_TS9	vB_AdhM_DL
NCBI accession	OP820700	OP820701	OP820702
Length	115,560 bp	115,503 bp	42,388 bp
Guanine-cytosine (G + C) content	41.10%	35.34%	34.43%
tRNAs (Ref= tRNAscan-SE v2.0)	30	-	-
Total CDS (Ref=Prokka v1.14)	151	195	75
Hypothetical proteins	121	175	66
Functional proteins (Ref = Blastp, E<10^{-5})	30	25	9
Virulence factor (Ref=VFDB)	-	-	-
Antimicrobial resistance genes (Ref = CARD)	-	-	-
Lysogenic markers (Ref = Blastp)	-	-	-
Lifestyle (Ref = PhageAI)	Virulent (99.10%)	Virulent (90.70%)	Virulent (91.21%)

Fig. 4. Genomic characterization of three bacteriophages targeting *A. dhakensis* AM, A) vB_AdhS_TS3 B) vB_AdhM_TS9 C) vB_AdhM_DL. Circles from outermost to innermost correspond to predicted genes (BLASTp, nr database, E value of ⟨10^{-5}) on the forward strand, reverse strand, and GC content.

Table 2
Features of the ORFs of three bacteriophages, predicted functions of proteins, and conserved domains detected.

ORF	start	stop	strand	Predicted function	Probability	E value	Conserved domain no.
phage vB_AdhS_TS3							
1	691	29	–	Hydrolase	99.74	1.60×10^{-16}	2GO7_C
3	2625	1045	–	UDP-2,3-diacylglucosamine hydrolase	98.95	2.30×10^{-8}	5K8K_A
15	7483	7596	+	Fimbrial protein	98.4	9.10×10^{-7}	4IXJ_B
29	13,672	12,083	–	Nicotinamide phosphoribosyltransferase	100	6.40×10^{-75}	8DSC_B
31	14,698	13,916	–	Ribose-phosphate pyrophosphokinase	100	2.00×10^{-38}	5MP7_A
32	14,979	14,695	–	Pyrophosphatase	98.22	2.80×10^{-5}	2GTA_C
52	22,228	21,368	–	Membrane protein	100	2.80×10^{-29}	7VHP_G
57	24,326	23,766	–	lemA protein	99.82	1.30×10^{-18}	2ETD_A
59	26,185	25,436	–	Serine/Threonine phosphatases	99.95	1.20×10^{-25}	1G5B_B
63	28,284	27,661	–	DNA polymerase III subunit epsilon	99.42	1.50×10^{-11}	5M1S_D
81	34,516	34,310	–	Thioredoxin glutathione reductase	98.23	7.60×10^{-5}	7B02_A
82	36,153	35,326	–	Putative ATP-dependent Clp protease proteolytic subunit	99.72	6.80×10^{-16}	1TG6_E
83	36,371	36,150	–	Deoxynucleoside monophosphate kinase	99.06	2.20×10^{-9}	1DEK_B
88	38,453	37,983	–	Ribonuclease H	99.73	5.90×10^{-15}	3H08_B
89	39,040	38,522	–	Dihydrofolate reductase	99.91	3.50×10^{-23}	3CSE_A
90	40,222	39,101	–	Ribonucleotide reductase R2	100	9.80×10^{-53}	1MXR_A
91	42,660	40,411	–	Ribonucleoside-diphosphate reductase 1 subunit alpha	100	1.80×10^{-113}	2XAP_C
93	43,815	43,324	–	Phosphate starvation-inducible protein	99.51	6.70×10^{-12}	3B85_A
94	44,031	43,831	–	RNA complex	98.27	2.20×10^{-6}	2XZO_A
100	48,501	46,093	–	DNA polymerase	100	4.80×10^{-73}	4XVK_A
102	48,947	48,792	–	DNA primase	98.24	3.40×10^{-6}	5VAZ_A
104	50,009	49,644	–	DnaB-like replicative helicase	99.39	4.70×10^{-11}	8DUE_B
109	51,631	51,071	–	snRNA-activating protein complex subunit 4	99.35	3.20×10^{-10}	7XUR_A
110	52,415	51,624	–	DNA ligase	99.97	8.80×10^{-29}	1DGS_B
111	53,608	52,598	–	DNA ligase	100	8.00×10^{-73}	4GLX_A
112	53,819	53,640	–	DNA binding protein	99.52	4.20×10^{-13}	5A4O_A
115	54,925	54,623	–	Homing endonuclease-DNA	99.42	4.30×10^{-13}	1A73_A
117	55,801	55,109	–	DNA binding protein	99.04	1.60×10^{-8}	2LVS_A
122	59,955	57,031	–	Eukaryotic initiation factor	99.77	2.00×10^{-16}	5ZC9_A
127	61,708	63,414	+	Anaerobic ribonucleotide-triphosphate reductase	100	1.70×10^{-54}	1HK8_A
129	63,875	64,339	+	Outer membrane protein A	99.43	4.60×10^{-11}	3NB3_B
136	66,830	67,258	+	Endonuclease V	100	5.40×10^{-43}	2END_A
152	69,872	70,051	+	Antitermination protein	97.97	1.60×10^{-5}	7UBN_Q
175	74,745	74,855	+	30S ribosomal protein	98.9	1.10×10^{-8}	2K4X_A
186	78,078	78,416	+	Circadian Clock Protein	98.81	3.30×10^{-8}	1R8J_B
187	78,413	79,444	+	Transcriptional regulator NadR	100	4.20×10^{-35}	1LW7_A
188	79,441	80,118	+	Nicotinamide riboside transporter	100	1.40×10^{-42}	4QTN_A
197	83,112	83,480	+	DNA binding protein	99.37	2.80×10^{-12}	2A1K_B
198	83,707	84,393	+	Nuclease SbcCD subunit D	99.66	8.20×10^{-15}	7DOG_B
204	86,807	87,541	+	Exodeoxyribonuclease	100	1.80×10^{-31}	5HML_B
205	87,726	88,226	+	Deoxyuridine 5′-triphosphate nucleotidohydrolase	99.95	3.00×10^{-25}	3MDX_A
209	89,272	89,156	–	Muramidase Lysozyme-like Peptidoglycan-binding	98.76	5.90×10^{-8}	6V3Z_B
210	89,551	89,420	–	Muramidase Lysozyme-like Peptidoglycan-binding	99.21	2.20×10^{-11}	6V3Z_B
218	93,068	92,955	–	Large tail fiber protein P34	98.11	8.60×10^{-6}	4UXF_C
224	95,866	95,729	–	Probable central straight fiber	98.97	6.50×10^{-10}	7ZQB_i
225	96,037	95,885	–	Probable central straight fiber	98.83	9.60×10^{-10}	7ZQB_i
228	97,213	97,067	–	Probable central straight fiber	99.72	3.00×10^{-18}	7ZQB_i
230	98,169	97,900	–	Baseplate	99.31	2.80×10^{-11}	8GTC_O
233	98,787	98,620	–	Tip attachment protein	99.04	5.10×10^{-10}	8IYK_J
234	99,393	98,908	–	Probable baseplate hub protein	99.66	1.90×10^{-15}	7ZHJ_c
238	100,667	100,473	–	Distal tail protein	99.06	1.30×10^{-9}	6F2M_C
253	106,959	106,681	–	Tail tube protein	99.51	7.40×10^{-14}	5NGJ_A
254	107,559	107,401	–	Tail tube protein	98.92	2.70×10^{-9}	5NGJ_A
258	109,315	109,010	–	Neck protein	99.46	1.10×10^{-12}	6TE9_C
259	110,749	109,370	–	Major capsid protein	100	1.10×10^{-30}	6TSU_J4
264	112,437	112,033	–	Portal protein	99.65	1.90×10^{-14}	8FQL_E
265	112,737	112,504	–	Portal protein	99.45	1.10×10^{-12}	8FQL_E
267	113,538	113,413	–	Terminase large subunit	98.47	4.60×10^{-7}	2WBN_A
phage vB_AdhM_TS9							
2	1373	516	–	HNH restriction endonuclease	98.93	6.00×10^{-9}	3M7K_A
3	2597	1494	–	RNA ligase	100	5.30×10^{-47}	6VTB_A
6	3846	3484	–	Deoxycytidylate deaminase	99.77	4.50×10^{-17}	2W4L_D
11	5550	5029	–	Ribonuclease HI	98.6	3.10×10^{-5}	2E4L_A
20	7598	8854	+	AAA ATPase	100	8.80×10^{-46}	8BNS_B
21	8871	10,661	+	DNA primase/helicase	100	1.70×10^{-53}	6N7I_D
22	10,673	12,955	+	DNA polymerase	100	1.30×10^{-50}	1X9M_A
23	13,082	13,474	+	HNH homing endonuclease	99.74	9.20×10^{-17}	1U3E_M
24	13,686	13,892	+	DNA polymerase	97.95	2.40×10^{-5}	1X9M_A
25	13,931	14,488	+	Helix-destabilizing protein	99.85	5.00×10^{-20}	1JE5_A
28	17,556	15,607	–	Tailspike protein	99.92	2.20×10^{-21}	6NW9_A
29	18,558	17,695	–	Ribosome	99.55	3.90×10^{-14}	7ANE_at
30	19,162	18,899	–	Ribosome	99.56	2.40×10^{-14}	7ANE_at
33	20,422	20,012	–	Tail fiber assembly protein	99.41	2.10×10^{-11}	5YVQ_B

(*continued on next page*)

Table 2 (*continued*)

ORF	start	stop	strand	Predicted function	Probability	E value	Conserved domain no.
35	21,764	21,150	–	Baseplate wedge protein	99.89	2.40×10^{-21}	7KH1_B2
36	23,276	21,777	–	Baseplate wedge protein	100	7.60×10^{-38}	7KH1_I5
38	26,234	25,623	–	Baseplate	99.82	5.30×10^{-19}	7YFZ_p
39	26,879	26,244	–	Baseplate	99.95	4.10×10^{-26}	4RU3_A
40	27,875	26,961	–	Baseplate	100	3.50×10^{-29}	8EON_E
41	28,289	27,963	–	Baseplate	99.92	5.90×10^{-24}	7YFZ_h
42	29,017	28,289	–	Baseplate complex	99.92	1.00×10^{-23}	7KH1_D3
45	32,552	31,395	–	DUF4379 domain-containing protein	99.85	1.40×10^{-20}	6YXX_E2
48	34,011	33,538	–	Sheath-tube	99.97	6.40×10^{-29}	8HDW_n
49	35,430	34,036	–	Tail sheath protein	100	4.90×10^{-57}	7KJK_C6
50	36,034	35,492	–	E217 gateway protein	99.94	6.60×10^{-25}	8FVH_b
51	36,463	36,044	–	Head completion protein	99.74	6.10×10^{-17}	7KJK_A4
55	39,046	38,006	–	Major capsid protein	100	2.90×10^{-35}	6XGP_B
56	39,443	39,066	–	Head decoration protein	99.71	5.70×10^{-16}	1TD4_A
59	42,170	41,184	–	DUF4379 domain-containing protein	99.67	3.30×10^{-16}	6YXX_E2
60	43,797	42,250	–	Portal protein	100	8.30×10^{-37}	5NGD_D
61	44,884	43,829	–	Large subunit terminase	99.75	1.20×10^{-16}	5OE8_B
62	45,891	45,199	–	HNH homing endonuclease	99.91	9.40×10^{-24}	1U3E_M
63	46,728	46,330	–	Large subunit terminase	99.42	2.60×10^{-12}	5OE8_B
65	48,423	47,194	–	DUF4379 domain-containing protein	99.9	1.80×10^{-23}	6YXX_E2
70	50,487	49,771	–	Serine/Threonine protein phosphatases	99.95	2.60×10^{-25}	1G5B_B
72	51,548	50,973	–	Phage terminase large subunit	99.78	4.30×10^{-17}	7KS4_B
76	54,958	53,627	–	Apicoplast DNA polymerase	99.47	1.30×10^{-12}	7SXQ_A
79	56,048	56,602	+	ATP-dependent protease subunit	99.6	3.80×10^{-14}	6KR1_J
89	60,225	61,226	+	DUF4379 domain-containing protein	99.66	8.90×10^{-16}	6YXX_E2
91	61,794	62,804	+	DUF4379 domain-containing protein	99.65	8.70×10^{-16}	6YXX_E2
95	63,585	64,844	+	DUF4379 domain-containing protein	99.9	4.70×10^{-23}	6YXX_E2
98	65,569	65,874	+	Putative pyrophosphohydrolase	99.67	4.80×10^{-15}	4YF1_C
101	66,802	68,175	+	DNA ligase	100	4.10×10^{-62}	6DT1_E
102	68,190	68,552	+	Hydrolase	99.4	3.70×10^{-11}	2Q73_B
107	69,697	70,458	+	HNH homing endonuclease	99.07	2.40×10^{-10}	1U3E_M
108	70,448	71,497	+	Ribonuclease H	99.94	1.00×10^{-25}	3H7I_A
116	73,445	74,005	+	Crossover junction endodeoxyribonuclease	99.93	1.00×10^{-23}	7XHJ_B
118	74,196	74,768	+	Recombination endonuclease VII	100	6.30×10^{-33}	1E7L_B
122	75,504	76,004	+	Spore cortex-lytic enzyme	99.93	5.70×10^{-24}	4F55_A
125	76,580	77,542	+	DNA polymerase III subunit epsilon	99.35	7.90×10^{-12}	5M1S_D
127	78,015	78,590	+	5′-Nucleotidase	99.88	4.80×10^{-21}	4L57_A
130	79,134	79,979	+	Thymidylate synthase	100	1.90×10^{-57}	3V8H_B
131	80,000	80,548	+	Dihydrofolate reductase	99.93	4.50×10^{-23}	8SSX_A
133	81,217	82,260	+	DUF4379 domain-containing protein	99.64	2.40×10^{-15}	6YXX_E2
138	83,439	85,700	+	Ribonucleoside-diphosphate reductase 1 subunit alpha	100	4.10×10^{-112}	2XAP_C
139	85,754	86,842	+	Ribonucleotide reductase	100	9.30×10^{-53}	1MXR_A
140	86,916	87,191	+	Circadian clock protein	99.01	3.50×10^{-8}	5JWO_B
141	87,288	89,378	+	Anaerobic ribonucleoside-triphosphate reductase	100	5.30×10^{-70}	8P28_A
142	89,375	89,848	+	Molybdenum cofactor biosynthesis protein A	99.45	9.10×10^{-13}	1TV8_A
148	92,147	92,887	+	Phosphate starvation-inducible protein	99.89	8.00×10^{-20}	3B85_A
155	95,869	96,417	+	lemA protein	99.85	1.00×10^{-19}	2ETD_A
158	97,221	98,105	+	Proteasome	99.61	4.40×10^{-14}	2JAY_A
196	114,449	113,181	–	Apicoplast DNA polymerase	99.55	1.30×10^{-13}	7SXQ_A
phage vB_AdhM_DL							
1	346	2	–	Major capsid protein	99.21	9.00×10^{-11}	7SJ5_A
2	743	366	–	Head decoration protein	99.72	2.80×10^{-16}	1TD4_A
4	2312	1827	–	Prohead core protein protease	92.43	3.9	5JBL_B
5	3470	2484	–	DUF4379 domain-containing protein	99.67	3.30×10^{-16}	6YXX_E2
6	5097	3550	–	Portal protein	100	8.30×10^{-37}	5NGD_D
7	6184	5129	–	Large subunit terminase	99.75	1.20×10^{-16}	5OE8_B
8	7191	6499	–	HNH homing endonuclease	99.91	9.90×10^{-24}	1U3E_M
9	8028	7630	–	Large subunit terminase	99.42	2.60×10^{-12}	5OE8_B
11	9729	8494	–	DUF4379 domain-containing protein	99.9	5.40×10^{-23}	6YXX_E2
16	11,787	11,071	–	Serine/Threonine protein phosphatases	99.95	2.60×10^{-25}	1G5B_B
18	12,848	12,273	–	Phage terminase large subunit	99.78	4.30×10^{-17}	7KS4_B
23	16,258	14,927	–	Apicoplast DNA polymerase	99.47	1.30×10^{-12}	7SXQ_A
26	17,348	17,902	+	ATP-dependent protease subunit	99.56	1.70×10^{-13}	6KR1_J
36	21,525	22,526	+	DUF4379 domain-containing protein	99.66	8.90×10^{-16}	6YXX_E2
38	23,094	24,104	+	DUF4379 domain-containing protein	99.65	7.10×10^{-16}	6YXX_E2
42	24,885	26,144	+	DUF4379 domain-containing protein	99.91	1.20×10^{-23}	6YXX_E2
44	26,496	26,726	+	DUF4379 domain-containing protein	99.91	1.20×10^{-23}	6YXX_E2
45	26,869	27,174	+	Putative pyrophosphohydrolase	99.66	5.40×10^{-15}	4YF1_C
48	28,102	29,475	+	DNA ligase	100	4.10×10^{-62}	6DT1_E
54	30,997	31,758	+	HNH homing endonuclease	99.07	2.40×10^{-10}	1U3E_M
55	31,748	32,797	+	Ribonuclease H	99.94	1.00×10^{-25}	3H7I_A
63	34,745	35,305	+	Crossover junction endodeoxyribonuclease	99.93	1.00×10^{-23}	7XHJ_B
65	35,496	36,068	+	Recombination endonuclease VII	100	5.60×10^{-33}	1E7L_B
69	36,804	37,304	+	Spore cortex-lytic enzyme	99.93	5.20×10^{-24}	4F55_A
72	37,880	38,842	+	DNA polymerase III subunit epsilon	99.35	1.10×10^{-11}	5M1S_D
74	39,315	39,890	+	5′-Nucleotidase	99.88	4.80×10^{-21}	4L57_A

(*continued on next page*)

Table 2 (*continued*)

ORF	start	stop	strand	Predicted function	Probability	E value	Conserved domain no.
77	40,434	41,279	+	Thymidylate synthase	100	1.80×10^{-57}	3V8H_B
78	41,300	41,848	+	Dihydrofolate reductase	99.93	4.50×10^{-23}	8SSX_A

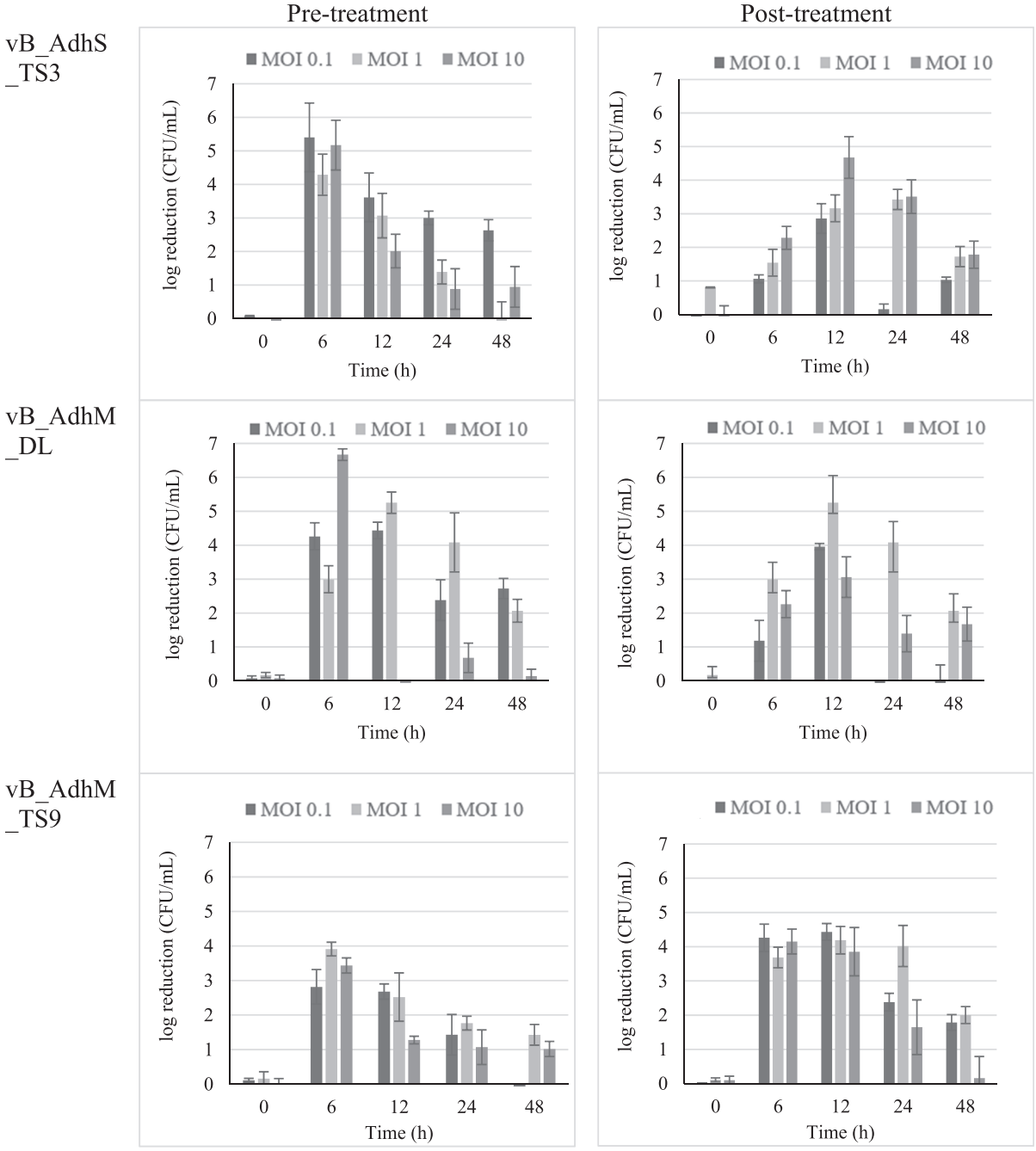

Fig. 5. The log reduction in *A. dhakensis* number in pre- and post-treatment using single phage vB_AdhS_TS3, vB_AdhM_DL and vB_AdhM_TS9. The data were expressed as mean ± SD. All assays were carried out in triplicates.

250 mL Erlenmeyer flask containing 50 mL of NB at 200 rpm and incubated at 30 °C for 48 h. For each assay, two control samples were set: the bacterial control and the phage control. The bacterial control was inoculated with *A. dhakensis* but not phages, and the phage controls were inoculated with phages but not bacteria. The control and test samples were incubated under the same conditions. Aliquots of the test samples and their controls were sampled at 0, 6, 12, and 24 h of incubation. In all assays, phage titer was determined in triplicate using the double-layer agar plate method. The bacterial concentration was determined in triplicate in the NA medium. Three independent experiments were performed for each condition.

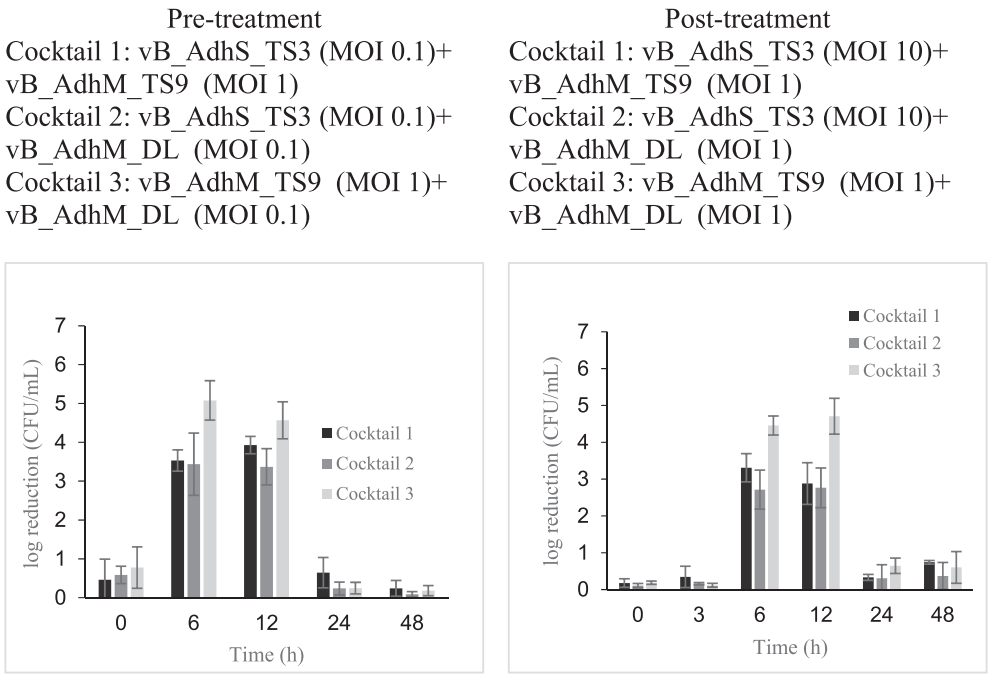

Fig. 6. The log reduction in *A. dhakensis* number in pre- and post-treatment groups using phage cocktail vB_AdhS_TS3, vB_AdhM_DL and vB_AdhM_TS9. The data are expressed as mean ± SD. All assays were carried out in triplicates.

2.11. A. dhakensis growth inhibition by phage cocktail and antibiotics combination

The inhibitory effects of the selected two-phage cocktail with effective MOIs in combination with antibiotics at sub-MIC (1/2 MIC) were determined as previously described. In the pre-treatment experiment, a combination of the selected two-phage cocktail with effective MOIs and amoxicillin at sub-MIC was added before inoculation with *A. dhakensis* AM (1×10^5 CFU/mL). In the post-treatment experiment, *A. dhakensis* AM suspensions (1×10^5 CFU/mL) were inoculated into NB and incubated for 3 h. Equal volumes of the selected three-phage cocktail with effective MOIs and amoxicillin at sub-MICs were added. Only the phage cocktail and antibiotics at MIC were also administered in both pre-and post-treatment. Phage and bacterial counts were determined in NB in two different volumes: 200 µL in 96-well microtiter plates and 20 mL in 250 mL Erlenmeyer flasks. The latter was incubated on an orbital shaker with a shaking speed of 200 rpm. After incubation at 30 °C, the aliquots of each sample and their controls were collected every 6 h for 48 h and were serially diluted to determine viable bacteria (CFU/mL) in NA plates incubated for 24 h at 30 °C.

2.12. Statistical analysis

Statistically significant differences in all experiments were determined by one-way analysis of variance (ANOVA), and post-hoc Tukey's test was applied to illustrate significant differences between bacterial concentrations between treatment groups over time. A p-value < 0.05 was considered to indicate statistical significance. SPSS statistical software package (version 13.0) was used for all analyses.

3. Results and discussion

3.1. Aeromonas isolation and identification

Three of the 40 isolates from 30 collection sites were preliminarily identified as *Aeromonas* by biochemical tests. These *Aeromonas* strains were then used as hosts for phage isolation. However, only the *Aeromonas* isolate AM was able to isolate phages using the enrichment technique. The isolated AM was further characterized using 16S rRNA gene sequencing, revealing a 99% identity with *A. dhakensis*. The neighbor-joining tree indicated that strain AM was most closely related to *A. dhakensis* (Fig. 1). The biochemical tests of *A. dhakensis* AM are shown in Table 1. To distinguish *A. dhakensis* from *A. hydrophila* subsp. *hydrophila* and *A. hydrophila* subsp. *ranae*, the results confirmed that strain AM was negative for L-arabinose and positive for salicin fermentation, confirming its classification as *A. dhakensis*. Furthermore, for more comprehensive characterization, a whole genome sequence analysis of strain AM was included in this study.

3.2. Antimicrobial susceptibility of A. dhakensis AM

The MICs of six antimicrobial agents against *A. dhakensis* AM were evaluated. Notably, amoxicillin had the highest MIC of 64 µg/mL among the antibiotics, a value significantly higher than the Clinical and Laboratory Standards Institute (CLSI) MIC breakpoints (>8 µg/mL) (data not shown). Considering the limited availability of information regarding the susceptibility profiles of *A. dhakensis*, our findings provide valuable insights into the antibiotic susceptibility of *A. dhakensis* AM. Specifically, our results demonstrate that *A. dhakensis* AM displays susceptibility to chloramphenicol, doxycycline, and gentamicin. Traditionally, *Aeromonas* have shown susceptibility to a range of antimicrobial agents, including 4th-generation cephalosporins, aminoglycosides, fluoroquinolones, tetracycline, and trimethoprim-sulfamethoxazole (Aravena-Roman et al., 2012). It is important to highlight that only a limited selection of antimicrobial agents, including oxytetracycline, amoxicillin, sulfadimethoxine/ormetoprim, and enrofloxacin, have been approved for use in aquaculture in Thailand (Baoprasertkul et al., 2012). Our results underscore the resistance rate to amoxicillin, in line with the report by Aravena-Roman et al. (2011), which noted that only 1.6% of 193 *Aeromonas* isolates were susceptible to amoxicillin. Recognizing the unique resistance pattern of amoxicillin against the target bacteria, we chose to incorporate amoxicillin at sub-MIC levels for our evaluation of synergism between the antibiotics and the phage cocktail. This choice was driven by the need to explore alternative treatment strategies given the observed resistance and to assess the potential of phages in complementing amoxicillin's limited efficacy in addressing *A. dhakensis* AM

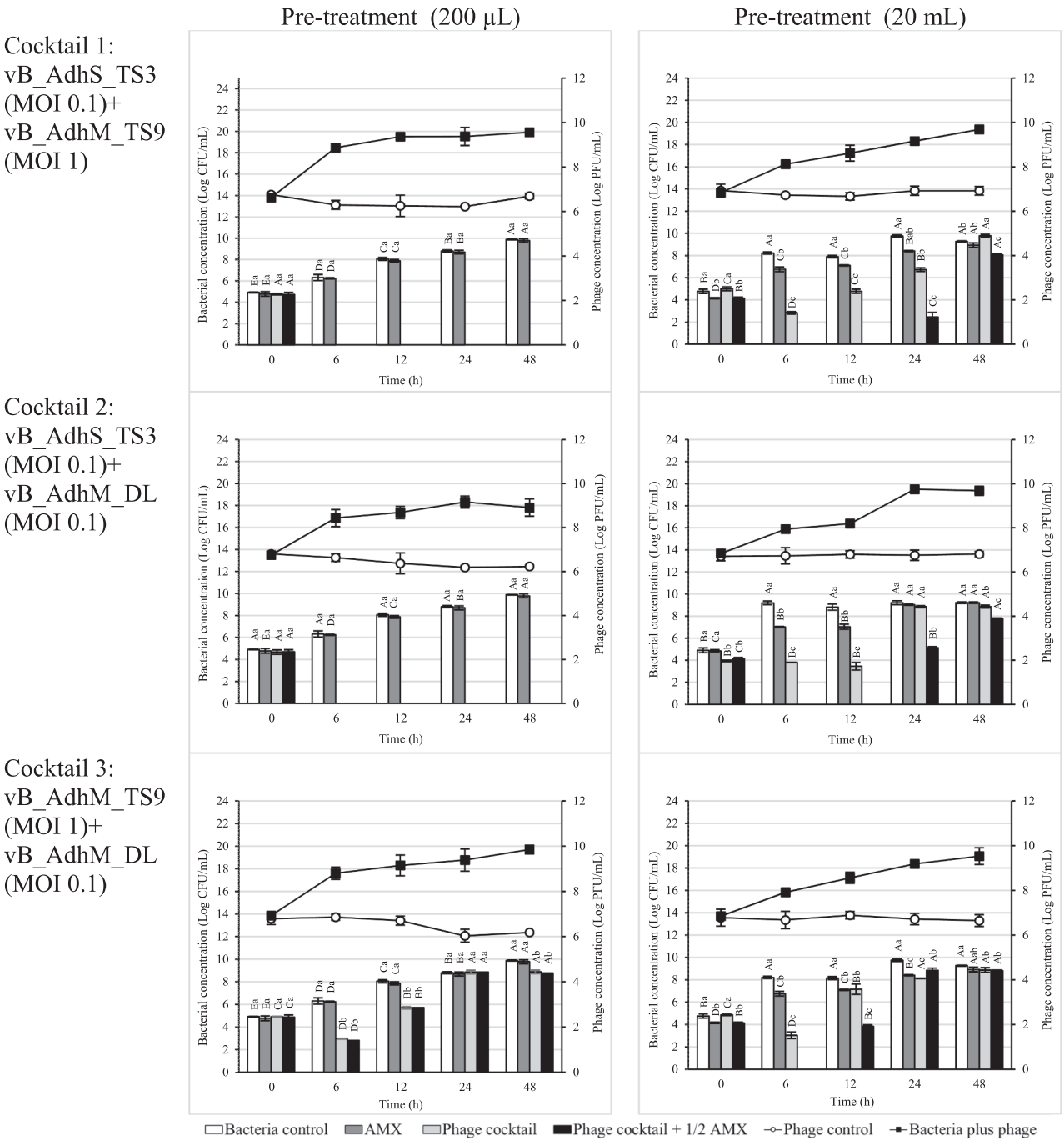

Fig. 7. Effect of phage cocktail and amoxicillin combination at 1/2 MIC against *A. dhakensis* AM. The bar graph represents the bacterial concentration (log CFU/mL), and the line graph represents the phage concentration (log PFU/mL). The data are expressed as mean ± SD. All assays were carried out in triplicates. Each lowercase label corresponds to a significantly different ($p < 0.05$) bacterial concentration within each time point. Capital letters denote significantly distinct ($p < 0.05$) bacterial concentrations and time points compared to each other time point within the same conditions.

infections.

3.3. Genomic features of A. dhakensis AM

The *in silico* genome of *A. dhakensis* AM comprises one circular chromosome of 4,884,279 bp with a G + C content of 61.9% (Fig. 2). The genome contained 4256 coding DNA sequences (CDSs). We emphasized the antimicrobial resistance genes and virulence factors corresponding to the main bacterial virulence determinants. Antimicrobial resistance genes were identified in the genome of *A. dhakensis* AM (Table S1). Virulence factor genes were identified in the genome of *A. dhakensis* AM (Table S2). Several typical toxin-encoding genes have been identified, such as aerolysin, hemolysin, and exotoxin. Five prophages were identified in the genome (Table S3), and no plasmids were found during genome analysis.

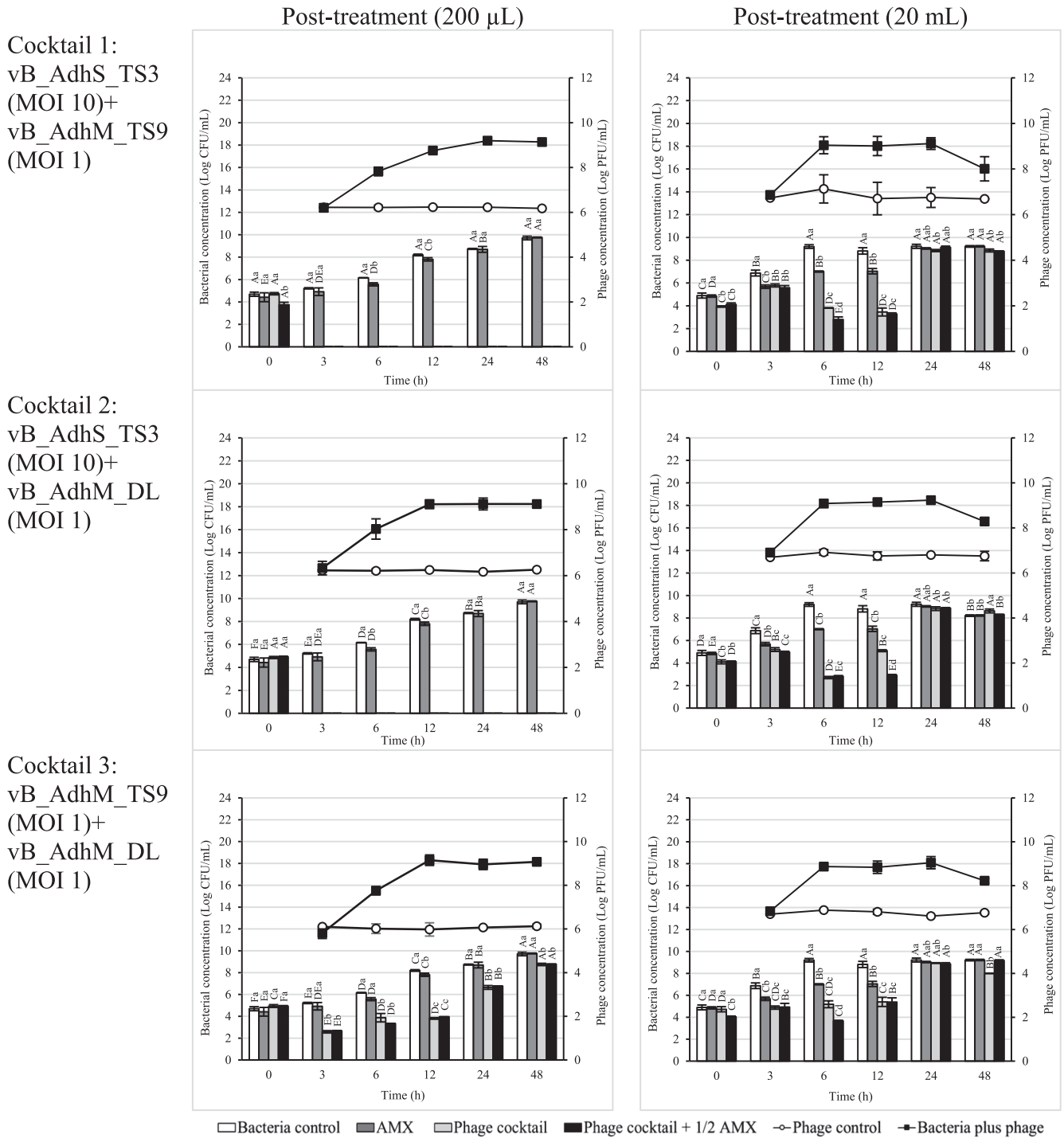

Fig. 7. (*continued*).

3.4. Phage isolation, purification and phage morphology

Four phages, designated as vB_AdhS_TS3, vB_AdhM_TS9, vB_AdhM_DL, and vB_AdhS_M4 were isolated using *A. dhakensis* AM as the host. These phages exhibited clear plaques with diameters ranging from 1.7 to 2.0 mm (Fig. 3). The electron micrographs revealed distinct morphologies for the isolated phages. Phage vB_AdhS_TS3 exhibited an icosahedral head of approximately 75.2 nm and a contractile tail with a length of 225.3 nm, while phage vB_AdhS_M4 had an icosahedral head of approximately 64.8 nm and a tail length of 185.4 nm. In contrast, phages vB_AdhM_DL and vB_AdhM_TS9 displayed different morphologies, with phage vB_AdhM_DL possessing an icosahedral head with dimensions of 50.4 nm and a tail length of 210.4 nm, and phage vB_AdhM_TS9 featuring an icosahedral head of approximately 85.1 nm and a shorter tail measuring 101.4 nm (Fig. 3). In a study by Bai et al. (2019), it was reported that among 51 complete genome sequences of *Aeromonas* phages in GenBank, the majority of *Aeromonas* phages were classified into different families. However, it's important to note that the ICTV's updated classification emphasizes that these morphological categories do not hold formal taxonomic significance in the classification of phages.

3.5. Host range determination

All phages were infected only with *A. dhakensis* and did not infect other *Aeromonas* spp., such as *A. hydrophila, A. caviae, A. sobria, A. trota*, or *A. veronii* (data not shown). Bacteriophage vB_AdhM_TS3 and vB_AdhM_TS9 are the broadest host range phage, able to infect *A. dhakensis* in five out of the six strains tested.

3.6. Optimal multiplicity of infection determination (MOI) and one-step growth curve

Phage vB_AdhS_TS3, vB_AdhM_DL, vB_AdhS_M4 and vB_AdhM_TS9 generated a maximum titre of 9.68 ± 0.05, 9.94 ± 0.05, 10.41 ± 0.06 and 8.85 ± 0.25 PFU/mL when infected at an optimal MOI of 10 (data not shown). The one-step growth curve of the phages revealed latent periods of approximately 40, 30, 50, and 30 min for vB_AdhS_TS3, vB_AdhM_DL, vB_AdhS_M4, and vB_AdhM_TS9, respectively. The burst sizes for these phages were estimated as 1380, 1280, 253, and 630 PFUs/infected cells, respectively (data not shown). Among the four phages, phage vB_AdhS_M4 had the longest latent period, smallest burst size, and narrowest host range. Therefore, we selected the other three phages, vB_AdhS_TS3, vB_AdhM_DL, and vB_AdhM_TS9, for further studies.

3.7. pH and thermal stability

All phages were resistant to a wide range of pH values after 2 h of incubation, and the optimum range was pH–6–8 (data not shown). No plaques were seen at pH 2. Regarding thermal stability, the phages maintained their stability relatively well after a 60-minute incubation at 4 °C, 25 °C, 30 °C, and 37 °C but were sensitive to higher temperatures (data not shown).

3.8. Whole genome sequencing and computational analyses

The genome size of vB_AdhS_TS3 was 115,560 bp with a G + C content of 41.10% (Fig. 4). The open reading frames (ORFs) of vB_AdhS_TS3 were identified with a total of 272 predicted ORFs. Among these genes, 58 were predicted to have known functions (Table 2, Fig. 4), and 184 ORFs were predicted to encode hypothetical proteins. Similarly, the genome size of vB_AdhM_TS9 was 115,503 bp, with a G + C content of 35.34%, and encoded 199 proteins. Out of 199 ORFs, 136 ORFs were hypothetical, whereas only 63 ORFs predicted functions (Table 2, Fig. 4). The genome size of vB_AdhM_DL was 42,388 bp, with a G + C content of 34.43% and 79 proteins, respectively. Of the 79 encoded proteins, Only 29 out of 79 encoded predicted functions, whereas 50 ORFs were hypothetical (Table 2, Fig. 4). We did not find an ORF encoding a protein with known toxins, antibiotic-resistant genes (ARGs), virulent factors (VFs) of bacterial origin, or lysogenic markers such as integrase, recombinase, repressor/anti-repressor protein, and excisionase in all three phage genomes.

3.9. Effect of single in pre- and post-treatment to control A. dhakensis AM growth

The lytic effect of individual phages on the growth of *A. dhakensis* AM was evaluated at different MOIs. Both pre-and post-treatment, the maximum cell decrease for all phages was observed during 6–12 h of incubation at all MOIs compared with the uninfected bacterial control. The pre-treatment with phages vB_AdhS_TS3, vB_AdhM_DL, and vB_AdhM_TS9 reduced the maximum bacterial count by 5.40, 6.67 and 3.91 log CFU/mL, respectively, after 6 h of incubation. In post-treatment, the maximum inactivation was achieved at 12 h with the log reduction number of 4.68, 5.25 and 4.43 log CFU/mL, respectively. The growth of bacteria cultured with phages decreased remarkably depending on the regrowth of bacteria at 48 h in all treatments (Fig. 5). When the phages were incubated in the presence of the host, the phages gradually increased and then became stable over 48 h of incubation. Based on the maximum inhibition, the combination of two phages as a phage cocktail in pre- and post-treatment with optimal MOIs was chosen, as shown in Fig. 6.

3.10. Effect of phage cocktail in pre- and post-treatment to control A. dhakensis AM growth

The effectiveness of the phage cocktail in the reduction of *A. dhakensis* AM is shown in Fig. 6. Cocktail 3, composed of phages vB_AdhM_TS9 and vB_AdhM_DL, was more effective against *A. dhakensis* AM than the other cocktails. Upon pre-treatment, the maximum inactivation with cocktail 3 (vB_AdhM_TS9 (MOI 1) + vB_AdhM_DL (MOI 0.1)) was 5.08 ± 0.51 log CFU/mL after 6 h of incubation compared with uninfected control. In post-treatment, the maximum reduction with cocktail 3 (vB_AdhM_TS9 (MOI 1) + vB_AdhM_DL (MOI 1)) was 4.71 ± 0.49 log CFU/mL after 12 h of incubation when compared with those of the bacterial control. Bacterial regrowth was observed at 24 h in all treatments. The phage alone was constant throughout the experiment. While phage cocktails hold promise in preventing the emergence of phage-resistant mutants, it's essential to acknowledge that prolonged incubation of phages and bacteria may lead to the development of phage-resistant strains (Malik et al., 2021). Another challenge in phage therapy is the high specificity of phages for their target bacteria. Each bacterial strain often requires a specific phage, and identifying the right phage for a particular infection can be a time-consuming process. In urgent or novel situations, this may not always be feasible. Thus, we have investigated the combination of phages with antibiotics as a strategy to mitigate potential limitations and expand the scope of treatment.

3.11. A. dhakensis growth inhibition by phage cocktail and antibiotics combination

To establish the phage-antibiotic synergy (PAS) effect, we determined the bacterial inactivation by three combinations of phage cocktails with amoxicillin at sub-MIC (32 μg/mL) in different volumes (200 μL and 20 mL). In the presence of amoxicillin and phage alone, the antibiotic- and phage-resistant variants rapidly grew after 6 h of incubation. In the pre-treatment, the combination of phage cocktail 1 or 2 with amoxicillin at sub-MIC resulted in complete inhibition during 48 h and 12 h in a volume of 200 μL and 20 mL, respectively (Fig. 7). At a volume of 20 mL, a significant reduction in bacterial numbers was observed when treated with a combination of phage cocktail 1 or 2 and sub-MIC amoxicillin at 48 h of incubation ($p < 0.05$). After post-treatment, the combination of phage cocktail 1 or 2 with amoxicillin at sub-MIC resulted in complete inhibition for 48 h in 200 μL (Fig. 7). However, only partial inhibition was observed after 12 h at a volume of 20 mL. Bacterial regrowth gradually increased after 12 h, and no significant reduction in viable bacteria was observed after 48 h of incubation compared to the phage cocktail of antibiotics alone. In this study, the bacterial concentration in this treatment (1×10^5 CFU/mL) was much higher than in natural bacterial contamination. Moreover, this study was performed in a higher volume of medium (20 mL), which may reduce the interaction between phages and/or antibiotics before reaching the bacteria. However, phage cocktails 1 and 2 decreased the CFU 1.2–1.7 log CFU/mL compared to the control and other groups treated individually after incubation for 48 h. Our study strongly suggests that the synergistic antibacterial effects of antibiotics and phages should be performed in the early stages when the bacterial number is low. The first use of the phage–antibiotic synergy (PAS) strategy was described by Comeau et al. (2007). Sublethal concentrations of antibiotics may help lytic bacteriophages reproduce rapidly and promote their antibacterial effects. Additionally, in combination with antibiotics, phages have multiple mechanisms to augment antibiotic effectiveness. They can break down bacterial biofilms using phage enzymes such as

depolymerases and lysins, rendering bacteria more susceptible to antibiotics (Liu et al., 2022b). Additionally, this combination therapy can reduce the likelihood of bacterial resistance development to both phages and antibiotics (Segall et al., 2019). Our study underscores the potential of phage-based approaches in combating *A. dhakensis* and demonstrates the efficacy of combination therapy utilizing phage cocktails and sublethal antibiotic concentrations. Furthermore, the ability of phages to target antibiotic-resistant strains, which are often challenging to treat with antibiotics alone, adds to the value of this approach. By focusing on *A. dhakensis*, we provide insights that extend to the broader challenge of antimicrobial resistance, emphasizing the importance of exploring innovative strategies to combat this critical global health issue.

Our study demonstrates that phage-based approaches are an attractive way to inactivate *A. dhakensis in vitro*. The cocktail of three different bacteriophages (phage vB_AdhS_TS3, vB_AdhM_DL and vB_AdhM_TS9) revealed promising *in vitro* lytic activity on *A. dhakensis*. Furthermore, the combination therapy using phage cocktails and antibiotics showed greater promise compared with either therapy alone. Moreover, combination therapy can also prevent the development of resistant mutants that would otherwise develop rapidly when exposed to antibiotics or phages. This demonstrates that using phages as an adjuvant with a sublethal concentration of antibiotics is an effective therapeutic strategy.

Declaration of Competing Interest

The authors declare that they have no known competing financial interests or personal relationships that could have appeared to influence the work reported in this paper.

Acknowledgements

This work was supported by Fundamental Fund (2021), Thailand Science Research and Innovation (TSRI) (grant number 031/2564), and graduate school fund, Faculty of Science, Srinakarinwirot University.

Appendix A. Supplementary data

Supplementary data to this article can be found online at https://doi.org/10.1016/j.jksus.2024.103111.

References

Adams, M.H., 1959. Bacteriophages. Interscience Publishers, New York.
Alcock, B.P., Raphenya, A.R., Lau, T.T., Tsang, K.K., Bouchard, M., Edalatmand, A., et al., 2020. CARD 2020: antibiotic resistome surveillance with the comprehensive antibiotic resistance database. Nucleic Acids Res. 48 (D1), D517–D525.
Aravena-Roman, M., Harnett, G.B., Riley, T.V., Inglis, T.J., Chang, B.J., 2011. *Aeromonas aquariorum* is widely distributed in clinical and environmental specimens and can be misidentified as *Aeromonas hydrophila*. J. Clin. Microbiol. 49 (8), 3006–3008.
Aravena-Roman, M., Inglis, T.J., Henderson, B., Riley, T.V., Chang, B.J., 2012. Antimicrobial susceptibilities of *Aeromonas* strains isolated from clinical and environmental sources to 26 antimicrobial agents. Antimicrob. Agents Chemother. 56 (2), 1110–1112.
Bai, M., Cheng, Y.-H., Sun, X.-Q., Wang, Z.-Y., Wang, Y.-X., Cui, X.-L., Xiao, W., 2019. Nine novel phages from a plateau lake in southwest China: insights into *Aeromonas* phage diversity. Viruses. 11 (7), 615.
Bankevich, A., Nurk, S., Antipov, D., Gurevich, A.A., Dvorkin, M., Kulikov, A.S., et al., 2012. SPAdes: a new genome assembly algorithm and its applications to single-cell sequencing. J. Comput. Biol. 19 (5), 455–477.
Baoprasertkul, P., Somsiri, T., Boonyawiwat, V., 2012. Use of veterinary medicines in Thai aquaculture: Current status. In: Bondad-Reantaso, M.G., Arthur, J.R., Subasinghe, R.P. (Eds.), Improving Biosecurity Through Prudent and Responsible Use of Veterinary Medicines in Aquatic Food Production. Rome, FAO, Italy, pp. 83–89.
Beaz-Hidalgo, R., Martinez-Murcia, A., Figueras, M.J., 2013. Reclassification of *Aeromonas hydrophila* subsp. *dhakensis* Huys et al., 2002 and *Aeromonas aquariorum* Martinez-Murcia et al., 2008 as *Aeromonas dhakensis* sp. nov. comb nov. and emendation of the species *Aeromonas hydrophila*. Syst. Appl. Microbiol. 36 (3), 171–176.
Bolger, A.M., Lohse, M., Usadel, B., 2014. Trimmomatic: a flexible trimmer for Illumina sequence data. Bioinformatics 30 (15), 2114–2120.
Brown, J., Pirrung, M., McCue, L.A., 2017. FQC dashboard: integrates FastQC results into a web-based, interactive, and extensible FASTQ quality control tool. Bioinformatics 33 (19), 3137–3139.
Carattoli, A., Zankari, E., Garcia-Fernandez, A., Voldby Larsen, M., Lund, O., Villa, L., Aarestrup, F.M., Hasman, H., 2014. PlasmidFinder and pMLST: *in silico* detection and typing of plasmids. Antimicrob. Agents Chemother. 58 (7), 3895–3903.
Cascon, A., Yugueros, J., Temprano, A., Sanchez, M., Hernanz, C., Luengo, J.M., Naharro, G., 2000. A major secreted elastase is essential for pathogenicity of *Aeromonas hydrophila*. Infect. Immun. 68 (6), 3233–3241.
Chen, P.L., Wu, C.J., Chen, C.S., Tsai, P.J., Tang, H.J., Ko, W.C., 2014. A comparative study of clinical *Aeromonas dhakensis* and *Aeromonas hydrophila* isolates in southern Taiwan: *A. dhakensis* is more predominant and virulent. Clin. Microbiol. Infect. 20 (7), O428–O434.
Clinical and Laboratory Standards Institute (CLSI), 2020. Performance standards for antimicrobial susceptibility testing of bacteria isolated from aquatic animals, third ed. Clinical and Laboratory Standards Institute, Wayne, PA.
Comeau, A.M., Tétart, F., Trojet, S.N., Prère, M.-F., Krisch, H.M., 2007. Phage-Antibiotic Synergy (PAS): β-lactam and quinolone antibiotics stimulate virulent phage growth. PLoS ONE 2 (8), e799.
Easwaran, M., Dananjaya, S.H.S., Park, S.C., Lee, J., Shin, H.-J., De Zoysa, M., 2017. Characterization of bacteriophage pAh-1 and its protective effects on experimental infection of *Aeromonas hydrophila* in Zebrafish (*Danio rerio*). J. Fish Dis. 40 (6), 841–846.
El-Araby, D.A., El-Didamony, G., Megahed, M., 2016. New approach to use phage therapy against *Aeromonas hydrophila* induced motile *Aeromonas* septicemia in Nile tilapia. J. Mar. Sci., Res. Dev. 6 (194), 2.
Figueras, M.J., Alperi, A., Saavedra, M.J., Ko, W.C., Gonzalo, N., Navarro, M., Martinez-Murcia, A.J., 2009. Clinical relevance of the recently described species *Aeromonas aquariorum*. J. Clin. Microbiol. 47 (11), 3742–3746.
Grant, J.R., Stothard, P., 2008. The CGView server: a comparative genomics tool for circular genomes. Nucleic Acids Res. 36 (2), W181–W184.
Huys, G., Kampfer, P., Albert, M.J., Kuhn, I., Denys, R., Swings, J., 2002. *Aeromonas hydrophila* subsp. *dhakensis* subsp. nov., isolated from children with diarrhoea in Bangladesh, and extended description of *Aeromonas hydrophila* subsp. Int. J. Syst. Evol. 52 (Pt 3), 705–712 hydrophila (Chester 1901) Stanier 1943 (approved lists 1980.
Janda, J.M., Abbott, S.L., 2010. The genus *Aeromonas*: taxonomy, pathogenicity, and infection. Clin. Microbiol. Rev. 23 (1), 35–73.
Jun, J.W., Kim, H.J., Yun, S.K., Chai, J.Y., Park, S.C., 2015. Genomic structure of the *Aeromonas* bacteriophage pAh6-C and its comparative genomic analysis. Arch. Virol. 160 (2), 561–564.
Lane, D.J., 1991. 16S/23S rRNA sequencing. In: Stackebrandt, E., Goodfellow, M. (Eds.), Nucleic Acid Techniques in Bacterial Systematics. Wiley, New York, pp. 115–175.
Liu, S., Lu, H., Zhang, S., Shi, Y., Chen, Q., 2022b. Phages against pathogenic bacterial biofilms and biofilm-based infections: a review. Pharmaceutics 14 (2), 427.
Liu, B., Zheng, D., Zhou, S., Chen, L., Yang, J., 2022a. VFDB 2022: a general classification scheme for bacterial virulence factors. Nucleic Acids Res. 50 (D1), D912–D917.
Malik, S., Nehra, K., Rana, J.S., 2021. Bacteriophage cocktail and phage antibiotic synergism as promising alternatives to conventional antibiotics for the control of multi-drug-resistant uropathogenic *Escherichia coli*. Virus Res. 198496.
Martinez-Murcia, A.J., Saavedra, M.J., Mota, V.R., Maier, T., Stackebrandt, E., Cousin, S., 2008. *Aeromonas aquariorum* sp. nov., isolated from aquaria of ornamental fish. Int. J. Syst. Evol. 58 (Pt 5), 1169–1175.
Pringsulaka, O., Patarasinpaiboon, N., Suwannasai, N., Atthakor, W., Rangsiruji, A., 2011. Isolation and characterization of a novel *Podoviridae*-phage infecting *Weissella cibaria* N22 from Nham, a Thai fermented pork sausage. Food Microbiol. 28, 518–525.
Puthucheary, S.D., Puah, S.M., Chua, K.H., 2012. Molecular characterization of clinical isolates of *Aeromonas* species from Malaysia. PLoS ONE 7 (2), e30205.
Seemann, T., 2014. Prokka: rapid prokaryotic genome annotation. Bioinformatics 30 (14), 2068–2069.
Segall, A.M., Roach, D.R., Strathdee, S.A., 2019. Stronger together? Perspectives on phage-antibiotic synergy in clinical applications of phage therapy. Curr. Opin. Microbiol. 51, 46–50.
Sunthornthummas, S., Doi, K., Rangsiruji, A., Sarawaneeyaruk, S., Pringsulaka, O., 2017. Isolation and characterization of *Lactobacillus paracasei* LPC and phage ΦT25 from fermented milk. Food Control. 73 (Pt 8), 1353–1361.
Yano, Y., Hamano, K., Tsutsui, I., Aue-Umneoy, D., Ban, M., Satomi, M., 2015. Occurrence, molecular characterization, and antimicrobial susceptibility of *Aeromonas* spp. in marine species of shrimps cultured at inland low salinity ponds. Food Microbiol. 47, 21–27.
Zhou, Y., Liang, Y., Lynch, K.H., Dennis, J.J., Wishart, D.S., 2011. PHAST: a fast phage search tool. Nucleic Acids Res. 39, W347–W352.